

HT2024-130842

THERMAL PERFORMANCE OF HOLLOW FLUID FILLED HEAT SINKS

John Nuszkowski, David Trosclair, Calla Taylor, Zaria Robins, and Steve Stagon
University of North Florida
Jacksonville, FL

ABSTRACT

The rapid advancement of technology and a continual increase in power density drive the need for lighter and more compact heat dissipation devices. The purpose of this research was to determine whether a hollow heat sink filled with fluid is more effective than solid heat sinks for heat dissipation. The copper and aluminum heat sinks consisted of a 4 x 4 fin array with an overall heat sink volume of 44.5 mm x 44.5 mm x 44.5 mm. The working fluids were water and acetone with a 50% fill volume for the hollow copper and aluminum heat sinks, respectively. Each heat sink was tested at nine operating points (varying applied heats and air velocities). The hollow copper heat sink had approximately the same overall heat sink thermal resistance while the hollow aluminum increased by 7% when compared to the solid copper heat sink and the hollow heat sinks had a 12% lower fin array thermal resistance. The weight was reduced by 82% and the mass based thermal resistance was 85% lower than the solid copper heat sink. The considerable decrease in mass without significant loss in thermal resistance demonstrates the potential widespread application across technologies requiring low-weight components.

Keywords: heat sink, heat pipe, heat spreader

NOMENCLATURE

A	cross sectional area
$\frac{dT}{dz}$	temperature gradient
k	thermal conduction coefficient
q	heat rate
R_a	fin array thermal resistance of the heat sink
R_b	base thermal resistance of the heat sink
R_t	total thermal resistance of the heat sink
$R_{t,m}$	mass based total thermal resistance of the heat sink
T_b	surface temperature at base of fin array
T_s	surface temperature at the top of the heater

T_∞	ambient air temperature
z	distance from the first heater temperature

1. INTRODUCTION

Heat dissipation devices, such as heat sinks, heat spreaders, and heat pipes, are essential in many applications to prevent component failure. The rapid advancement of technology and a continual increase in power density drive the need for lighter and more compact heat dissipation devices. Heat sinks are a form of heat dissipation device that transfers the heat generated from a device into either air or fluid, typically through large surface areas. Heat pipes are thermal transfer devices with high heat transfer capabilities through the phase-change of a working fluid.

Heat sinks have five categories: Passive, semi-active, active, liquid-cooled cold plates, and phase change recirculating system [6] with different heights and load limitations. There are also five types of heat sinks: stampings, extrusions, bonded/fabricated fins, castings, and folded fins [6]. Each type of heat sink has its own characteristics. Stampings have copper or aluminum sheets stamped into the necessary shapes [6]. Extrusions can be cut by machines, and have additional pieces added to them; crosscutting gives an omnidirectional rectangular heat sink [6]. Bonded/fabricated fins are high-performance and use aluminum-filled epoxy to attach finds to a base plate. Casting involves using a die-casting process (with or without vacuum sealing) inside of aluminum, copper, or bronze [6]. Lastly, folded fins use corrugated sheet metal (usually aluminum or copper) to create the fins, then they are attached to a base plate or directly to the heating surface [6]. Each of these types has its own efficiencies.

Heat sinks work very well transporting heat, but extreme temperatures will limit their dissipation abilities; if a heat sink's fins are too fragile or damaged, heat will not dissipate [2]. Therefore, heat sinks and heat pipes together are beneficial. Heat pipes allow for flexibility when there are contact areas with heat sources and heat sinks [2]. Heat pipes are heat transfer devices

with high efficiency and high heat transfer capabilities. They consist of three parts: an evaporator, condenser, and adiabatic section. Each of these sections work together to transfer heat from one end of the pipe to the other. The evaporator absorbs heat and evaporates the working fluid, which then goes through the condenser. The condenser makes the working fluid liquid again, and the liquid goes back through the evaporator.

Heat pipes are typically used in three ways: temperature equilibrium, temperature control, and separation of a heat source and sink [2]. They are heavily used in many computer systems, due to the high-power requirements leading to a high heat emission; these pipes act as a cooling system [2]. To use the heat pipe with the electronic system, there are two options: mounting the system directly onto the heat pipe or mounting it to a plate that has heat pipes inside of it [2].

Typically, the working fluids in heat pipes are water, ethanol, methanol, and acetone [1]. If ethanol, methanol, or acetone is used, it is usually mixed with water; a study conducted by Zamani et al. showed that a ratio of 1:3 ethanol-water mixture had the best thermal performance, as did water-acetone mixtures with a ratio of 4:1, 1:1, 1:4, and 1:13 [1].

There are many sizes of heat pipes; however electronic devices usually use small or micro heat pipes (MHP) due to space limitations. MHPs are small-scale devices with a length of only a few centimeters, and a diameter of about 100 μ [2]. Currently, micro heat pipes are made by using micromachining tech. (MEMS) and are tested to ensure that the pipe can act as a thermal heat spreader [2]. Hung and Seng investigated the performance of different star groove geometries on MHPs.

The rapid advancement of technology and a continual increase in power density drive the need for lighter and more compact heat dissipation devices. The purpose of this research is to determine whether a hollow fluid-filled (FF) heat sink is more effective than solid heat sinks for heat dissipation.

2. MATERIALS AND METHODS

2.1 Heat Sinks

The four heat sinks were constructed as 4x4 fin arrays (Fig. 1 and 2). Two heat sinks were solid metal: one solid copper and one solid aluminum. The other two heat sinks were hollow. The thermal properties of the copper and aluminum are shown in Table 1. The hollow heat sinks consisted of three pieces: bottom plate, hollow base and fins, and a fill tube. The copper bottom plate and fill tube (inserted at the top of one fin) were soldered to the hollow copper base and fins. On the hollow aluminum heat sink, the bottom plate and fill tube were welded and epoxied, respectively. It should be noted that the hollow base had a wall thickness of 1.25 mm, and the hollow fins had an internal bore diameter of 4.6 mm. The hollow copper and aluminum sinks were vacuum sealed and filled with fluid with a fill volume of 50%. Water was used in the hollow copper heat sink and acetone was chosen for the hollow aluminum heat sink to prevent corrosion and outgassing.

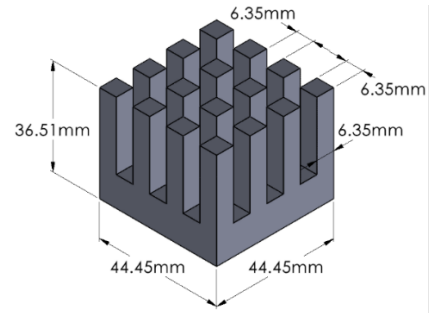


FIGURE 1: SOLID COPPER AND ALUMINUM HEAT SINK

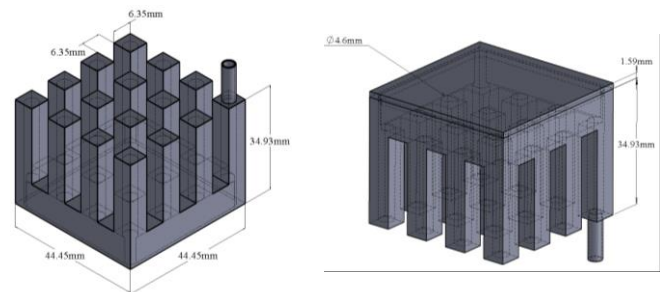


FIGURE 2: FLUID-FILLED COPPER AND ALUMINUM HEAT SINK

TABLE 1: THERMOPHYSICAL PROPERTIES

Property	Units	CU ¹	AL ²
Density	kg/m ³	8933	2702
Specific Heat	J/kg-K	385	934
Thermal Conductivity	W/m-K	401	195

¹ At 27 °C

² At 75 °C

2.2 Experimental Testing Apparatus

The experimental testing apparatus to evaluate and assess the performance of a heat pipe integrated with a conventional heat sink included a wind tunnel with a fan, an aluminum heater block, Arduino microcontrollers, and a heat source (Fig. 3 and 4). Power is supplied to the bottom of the heating block and applies a heat of 20 W, 40 W, and 60 W to the base of the heat sink. Four thermistor sensors, with an accuracy of ± 0.25 °C, were used to measure temperature at 6.4 mm and 57.2 mm from the top of the aluminum heater block, at the base of the fins, and the tip of a fin (Figure 3). The fin base and fin tip temperature sensors were applied with thermal paste and conductive copper or aluminum tape for their respective heat sinks. The fan power supply interfaces with the fan to modulate the velocity through the wind tunnel. To measure air velocity, a thermopile-based air velocity sensor was located inside the wind tunnel with an accuracy of ± 0.36 m/s. Each heat sink had the same thermal paste applied between the top surface of the heater block and the bottom surface of the heat sink.

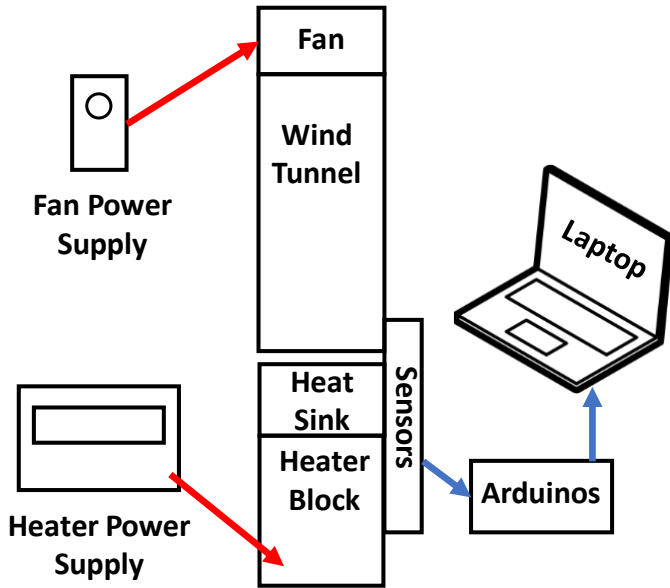


FIGURE 3: EXPERIMENTAL APPARATUS SCHEMATIC

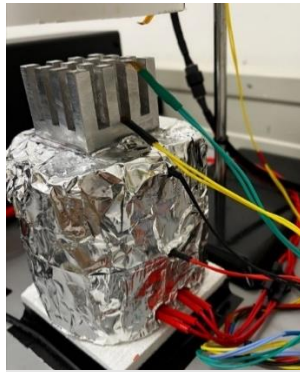


FIGURE 3: TEMPERATURE SENSOR LOCATIONS

2.3 Experimental Procedure

Each heat sink was tested at nine different operating conditions with three distinct heat inputs and corresponding velocities (Table 2). Each operating condition was conducted for 3600 s to reach steady state. The steady state condition was then measured and recorded over five minutes.

TABLE 2: THERMOPHYSICAL PROPERTIES

Heater Power (W)	Air Velocity (m/s)
20	0.0, 2.5, 5.0
40	2.0, 3.5, 5.0
60	4.0, 4.5, 5.0

2.4 Theory

The heat transfer rate into the heat sinks was calculated using Fourier's Law (Eq. 1) using the two measured temperatures along the heater block and distance between the

temperature sensors. Equation 1 neglects heat loss through the sides of the heater block. The total thermal resistance was determined from the heat transfer rate and the difference between the heater top surface and ambient temperature (Eq. 2). This resistance includes the thermal interface resistance between the top surface of the heater block and the bottom surface of the heat sink. The top surface of the heater was extrapolated assuming a linear temperature distribution along the heater block and using the two measured temperatures. The thermal resistance for the fin array and base of the heat sink were calculated using Eq. 3 and 4, respectively. Additionally, to account for the significant weight difference between the four heat sinks, a mass based total thermal resistance was calculated using Eq. 5. Therefore, a lighter weight heat sink with the same thermal resistance will have a lower mass based thermal resistance.

$$q = -kA \frac{dT}{dz} \quad (1)$$

$$R_t = \frac{(T_s - T_\infty)}{q} \quad (2)$$

$$R_a = \frac{(T_b - T_\infty)}{q} \quad (3)$$

$$R_b = R_t - R_a \quad (4)$$

$$R_{t,m} = m * R_t \quad (5)$$

3. RESULTS

The transient tests reached steady state after 1 hour when the average change in the heater block temperature was less than 0.002 K/s. As an example, Fig. 4 shows the transient test for the top surface of the heater for the hollow copper heat sink at a heat transfer rate of 60 W and air velocity of 5 m/s. It should be noted that calculated thermal resistances from Eq. 3, 4, and 5 changed by less than 1% after 50 minutes. The measured and extrapolated steady state temperatures for all the heat sinks at heat transfer rate and air velocity of 60 W and 5 m/s, respectively, are shown in Fig. 5. The two measured heater block temperatures, extrapolated top heater surface temperature, measured fin base temperature, and measured fin tip temperature are labeled. A distance of zero corresponds to the location of the heater temperature closest to the heaters. The two measured heater temperatures were used in Eq. 1 to calculate the change in temperature with distance for Fourier's Law. The same two temperatures were used to extrapolate the temperature at the top surface of the heater used in Eq. 2. The fin base and fin tip temperatures were directly measured and labeled in Figure 5.

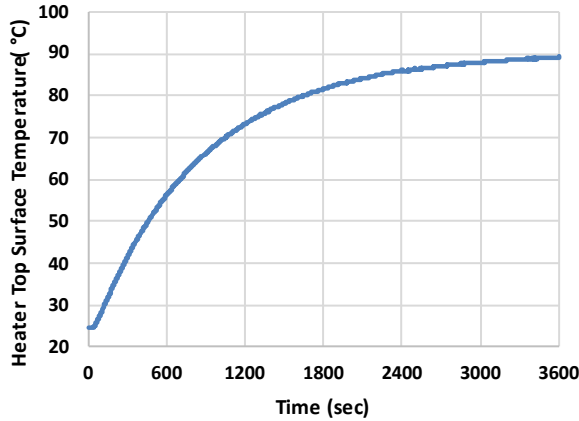


FIGURE 4: TRANSIENT TEST RESULTS OF THE TOP SURFACE OF THE HEATER FOR THE HOLLOW COPPER HEAT SINK AT A HEAT RATE OF 60 W AND AIR VELOCITY OF 5 M/S

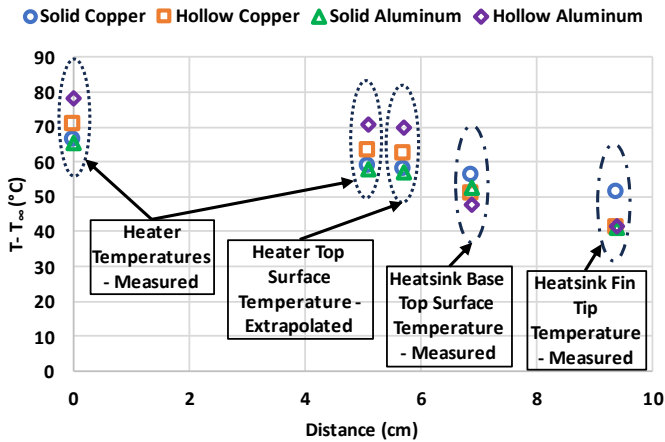


FIGURE 5: STEADY STATE TEMPERATURE DIFFERENCES FOR THE HEAT SINKS AT A HEAT RATE OF 60 W AND AIR VELOCITY OF 5 M/S

At a heat rate of 20 W, the total thermal resistances (Eq. 2) decreased with the FF copper heat sink by 1 to 5% compared to the solid copper heat sink (Fig. 6). The FF copper heat sink changed the total thermal resistance by -3 to 1% compared to the solid copper heat sink. At the highest heat rate of 60 W, the total thermal resistance increased by 4 to 6% with FF copper heat sink compared to the solid copper heat sink. The mean of all nine operating points for the total thermal resistance of the FF copper heat sink was within 0.4% of the solid version. While the total thermal resistance increased or decreased depending on the operating point, the thermal resistance for the fin array (Eq. 3) decreased at all operating points for the FF copper heat sink compared to the solid copper heat sink (Fig. 7). The decrease in fin array thermal resistance was 8 to 15 % with an average decrease of 12%.

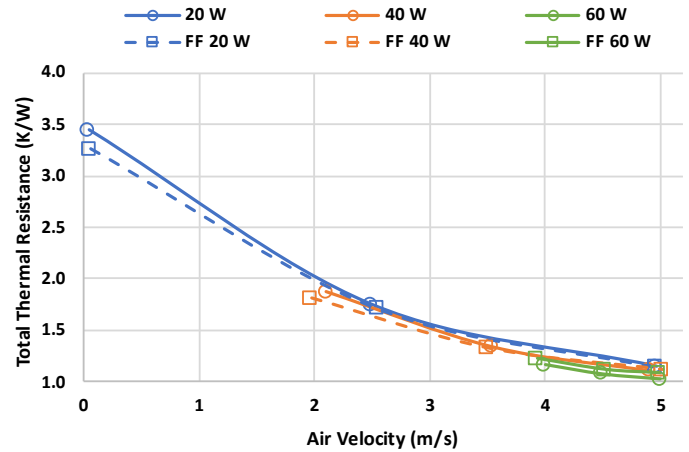


FIGURE 6: TOTAL ARRAY THERMAL RESISTANCE AT VARYING HEAT TRANSFER RATES AND AIR VELOCITIES FOR THE SOLID AND FF COPPER HEAT SINKS

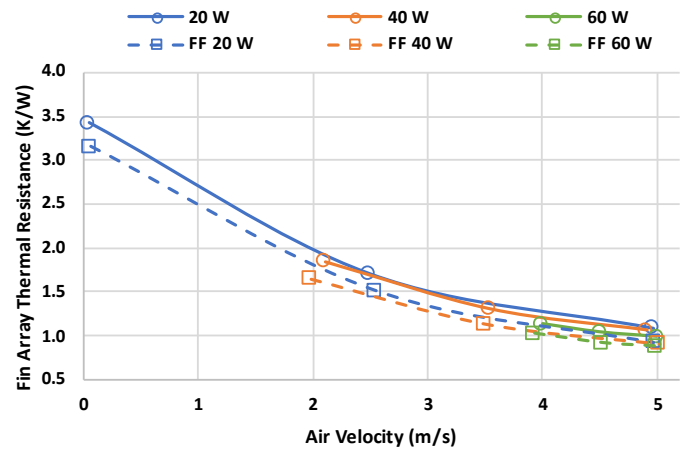


FIGURE 7: FIN ARRAY THERMAL RESISTANCE AT VARYING HEAT TRANSFER RATES AND AIR VELOCITIES FOR THE SOLID AND FF COPPER HEAT SINKS

The total thermal resistance (Eq. 2) for the FF aluminum heat sink increased (Fig. 8) at every operating point compared to the solid aluminum heat sink except at a heat rate of 20 W with still air (air velocity of 0 m/s). The change in total thermal resistance varied from a decrease of 4% to an increase of 22% for the FF compared to the solid aluminum heat sink with an average increase of 10%. As with the copper heat sinks, the fin array thermal resistance (Eq. 3) decreased at all operating points for the aluminum FF heat sink compared to the solid aluminum heat sink. The decrease in fin array thermal resistance varied from 6 to 16% with an average of decrease of 12%.

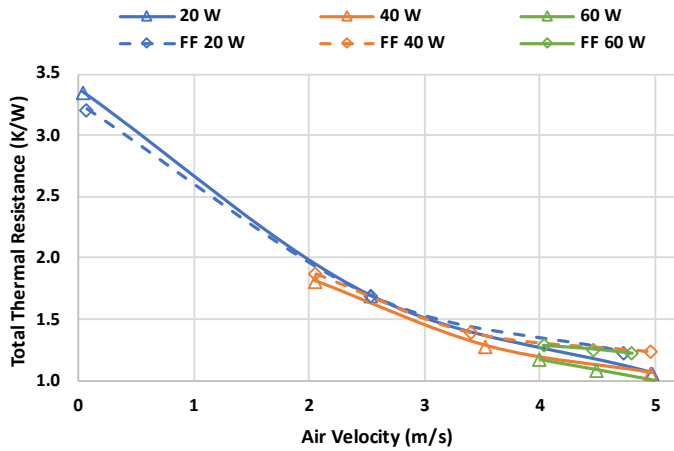


FIGURE 8: TOTAL ARRAY THERMAL RESISTANCE AT VARYING HEAT TRANSFER RATES AND AIR VELOCITIES FOR THE SOLID AND FF ALUMINUM HEAT SINKS

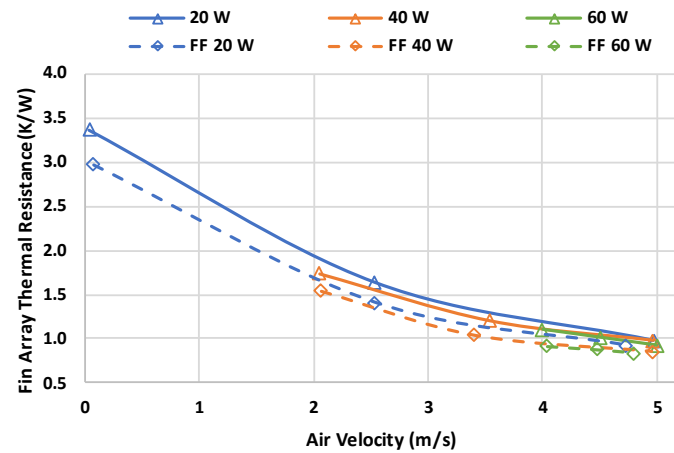


FIGURE 9: FIN ARRAY THERMAL RESISTANCE AT VARYING HEAT TRANSFER RATES AND AIR VELOCITIES FOR THE SOLID AND FF ALUMINUM HEAT SINKS

4. DISCUSSION

As shown in Fig. 7 and 9, the fin array thermal resistance (Eq. 3) decreased for the FF heat sinks compared to their solid versions. In addition, the fin array thermal resistance for the FF copper or FF aluminum heat sink was less than the solid copper or aluminum heat sinks with the FF aluminum heat sink having the lowest thermal resistance for the fin array (Fig. 10). The total thermal resistance was the sum of the base and fin array thermal resistances (Eq. 4). The varying total thermal resistance from the FF heat sinks can be attributed to their increase in base thermal resistance (Fig. 11). The FF aluminum heat sink had the highest base thermal resistance. Decreasing the height of the base should decrease the base thermal resistance. This increase in base thermal resistance may be due to unfavorable fluid motion within the base volume of the heat sink.

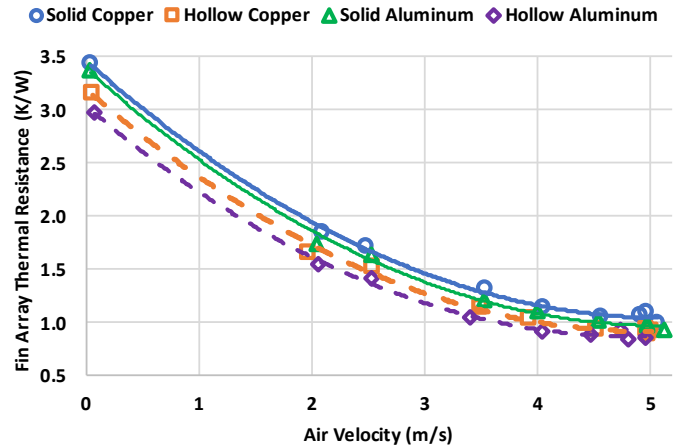


FIGURE 10: FIN ARRAY THERMAL RESISTANCE AT VARYING VELOCITIES FOR ALL THE HEAT SINKS

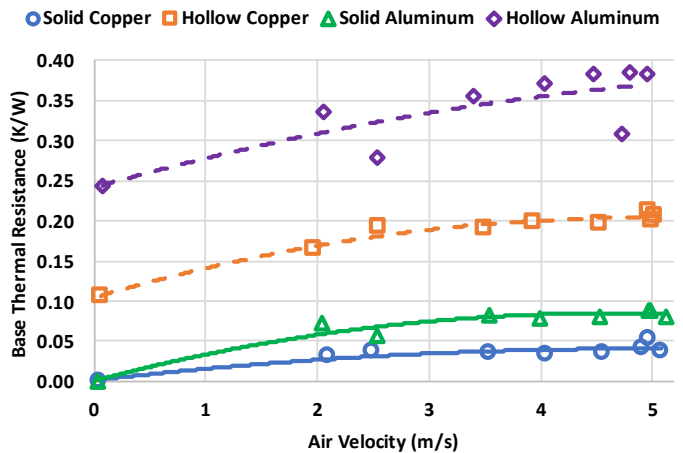


FIGURE 11: HEAT SINK BASE THERMAL RESISTANCE AT VARYING VELOCITIES FOR THE HEAT SINKS

As shown in Table 1, copper has 2.1 times the thermal conductivity of aluminum, but 3.3 times the density. The FF copper and aluminum heat sinks had a reduction in mass of 40% and 43% to their solid versions. In addition, the FF aluminum heat sink had an 82% reduction in mass compared to the solid copper heat sink. On average, the total thermal resistance of the FF aluminum heat sink increased by 7% compared to the solid copper heat sink. To incorporate the thermal resistance and mass of the heat sink, a mass based thermal resistance was defined (Eq. 5). Figure 12 shows the mass based thermal resistance for all the heat sinks. The FF aluminum heat sink had the lowest mass based thermal resistance and was, on average, 85% lower than the solid copper heat sink. FF heat sinks can provide a lightweight option for industries, such as space, automotive, and military applications.

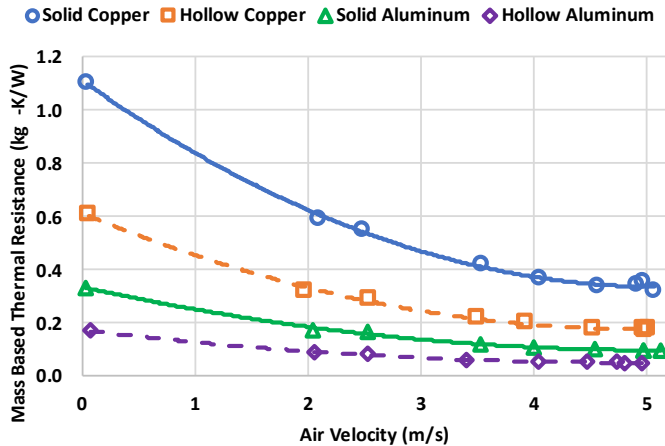


FIGURE 12: MASS BASED THERMAL RESISTANCE AT VARYING VELOCITIES FOR THE HEAT SINKS

5. CONCLUSION

This study designed, developed, and tested a hollow copper heat sink filled with 50% water (by volume) and a hollow aluminum heat sink filled with 50% acetone (by volume) and compared the two heat sinks to solid versions of the copper and aluminum heat sinks. The need for improved heat dissipation devices is evident due to the increasing power densities of electronics. Each heat sink was tested at nine different operating conditions with different heat transfer rates and air velocities using an experimental test apparatus developed in-house. The total thermal resistances of the heat sinks, which was the heat sink base plus the heat sink fin array thermal resistances, were compared at the different operating conditions. In addition, a mass based thermal resistance was compared to illustrate the significantly different masses between copper, aluminum, hollow copper, and hollow aluminum. The main conclusions are shown below.

- The total thermal resistance of the copper FF heat sink compared to the solid copper heat sink ranged from -5% to 6 % increase with an average increase in total thermal resistance of 0.4%.
- The copper FF heat sink decreased the fin array thermal resistance by 8 to 15 % with an average decrease of 12% compared to the solid copper heat sink.
- The total thermal resistance for the aluminum FF heat sink varied from a decrease of 4% to an increase of 22% with an average increase of 10% compared to the solid aluminum heat sink.

- The aluminum FF heat sink decreased the fin array thermal resistance by 6 to 16% with an average decrease of 12% compared to the solid aluminum heat sink.
- The varying total thermal resistance from the FF heat sinks can be attributed to their increase in base thermal resistance. Decreasing the height of the base should decrease the base thermal resistance.
- The total thermal resistance of the FF aluminum heat sink increased by 7% compared to the solid copper heat sink, but the FF aluminum heat sink had an 82% reduction in mass compared to the solid copper heat sink.
- The FF aluminum heat sink had the lowest mass based thermal resistance and was, on average, 85% lower than the solid copper heat sink.

ACKNOWLEDGEMENTS

This study was supported by the University of North Florida (UNF) School of Engineering. The authors would also like to acknowledge the support of undergraduate students Mason Lovelace and George Wolfe in fabrication of the heat sinks.

REFERENCES

- [1] Y. Xu, Y. Xue, H. Qi, and W. Cai, "An updated review on working fluids, operation mechanisms, and applications of pulsating heat pipes," *Renewable and Sustainable Energy Reviews*, vol. 144, pp. 1–34, Mar. 2021.
- [2] BAHMAN ZOHURI, *Heat Pipe Design and technology: Modern applications for practical thermal management*. Albuquerque, NM: SPRINGER, 2018.
- [3] X. Chen, H. Ye, X. Fan, T. Ren, and G. Zhang, "A review of small heat pipes for Electronics," *Applied Thermal Engineering*, vol. 96, pp. 1–17, Nov. 2015.
- [4] T. Q. Feng and J. L. Xu, "An analytical solution of thermal resistance of cubic heat spreaders for electronic cooling," *Applied Thermal Engineering*, vol. 24, no. 2-3, pp. 323–337, Sep. 2003.
- [5] S.-S. Hsieh, R.-Y. Lee, J.-C. Shyu, and S.-W. Chen, "Thermal performance of flat vapor chamber heat spreader," *Energy Conversion and Management*, vol. 49, no. 6, pp. 1774–1784, Feb. 2008.
- [6] S. Lee, "Optimum design and selection of heat sinks," *Proceedings of 1995 IEEE/CPMT 11th Semiconductor Thermal Measurement and Management Symposium (SEMI-THERM)*, pp. 812–817, Dec. 1995.